Accelerated Publication

THE JOURNAL OF BIOLOGICAL CHEMISTRY
Vol. 276, No. 32, Issue of August 10, pp. 29621–29624, 2001

An Enhanced Mutant of Red Fluorescent Protein DsRed for Double Labeling and Developmental Timer of Neural Fiber Bundle Formation*

Received for publication, April 17, 2001, and in revised form, June 11, 2001
Published, JBC Papers in Press, June 14, 2001,
DOI 10.1074/jbc.C100200200

Vladislav V. Verkhusha‡§, Hideo Otsuna¶‖, Takeshi Awasaki¶ **, Hiroki Oda‡, Shoichiro Tsukita‡ ‡‡, and Kei Ito¶ **

*From the ‡Tsukita Cell Axis Project, Exploratory Research for Advanced Technology (ERATO), Japan Science and Technology Corporation (JST), Kyoto Research Park, Kyoto 600-8813, ¶National Institute for Basic Biology, Okazaki 444-8585, ‖Division of Biological Science, Nagoya University, Nagoya 464-8602, ‡‡Department of Cell Biology, Faculty of Medicine, Kyoto University, Kyoto 606-8501, and **Precursory Research for Embryonic Science and Technology (PRESTO), JST, Okazaki 444-8585, Japan*

We developed a new variant of coral-derived red fluorescent protein, DsRed S197Y, which is brighter and essentially free from secondary fluorescence peak. This makes it an ideal reporter for double labeling with green fluorescent protein (GFP). Though purified protein shows only 20% stronger fluorescence emission, culture cells that express DsRed S197Y exhibit a 3–3.5 times higher level of fluorescence than the cells that express wild-type DsRed. The much slower fluorescence maturation of DsRed than that of GFP is a beneficial feature for a fluorescent developmental timer application. When GFP and DsRed S197Y are expressed simultaneously, emissions start at different latency. This provides information about the time after the onset of expression. It reflects the order of cell differentiation if the expression is activated upon differentiation of certain types of cells. We applied this system to the developing brain of *Drosophila* and visualized, for the first time, the formation order of neural fibers within a large bundle. Our results showed that newly extending fibers of the mushroom body neurons mainly run into the core rather than to the periphery of the existing bundle. DsRed-based timer thus presents an indispensable tool for developmental biology and genetics of model organisms.

The coral-derived red fluorescent protein DsRed (1, 2), with its significantly red-shifted excitation and emission maxima (558 and 583 nm, respectively), has attracted tremendous interest because of its good complementation to the green fluorescent protein (GFP)[1] and its enhanced mutants (3). DsRed, however, has a relatively low emission level and a parasitic green fluorescence peak that cross-talks with GFP emission (4). In GFP, a mutation at the 203rd amino acid residue (corresponding to position 197 in DsRed), which is in close contact with chromophore (5), to aromatic amino acid is mainly responsible for the enhancement of extinction coefficient and fluorescence shift to a longer wavelength (5, 6). Following this idea, we performed a round of DsRed mutagenesis and obtained an enhanced variant, DsRed S197Y, in that Ser-197 is converted to Tyr. We analyzed its expression and maturation in heterologous systems of bacteria, insect, and mammalian cells, and further demonstrated its usage in *Drosophila* to monitor activation of target promoters and cell differentiation on the whole organism scale.

EXPERIMENTAL PROCEDURES

Construction of DsRed S197Y and the Transgenic Drosophila Strain—The 0.71-kb *Nde*I-*Bam*HI fragment of wild-type DsRed and 0.75-kb *Nco*I-*Bam*HI fragment of EGFP were amplified by PCR from pDsRed1-N1 and pEGFP-N1 plasmids (CLONTECH) and subcloned into pET-11c and pET-11d vectors (Invitrogen). Polyhistidine tags were added to C termini during PCR amplification. Resulted pET-11c-DsRed-Hisx6 and pET-11d-EGFP-Hisx6 plasmids were transfected into *Escherichia coli* BL21(DE3) host (Invitrogen). Mutation Ser-197 to Tyr (S197Y) was introduced into pET-11c-DsRed-Hisx6 using a transformer site-directed mutagenesis kit (CLONTECH). The PCR-amplified cDNAs of DsRed and DsRed S197Y were inserted into *Kpn*I-*Xba*I sites of pUASp vector (7), resulting in pUASp-DsRed and pUASp-DsRed S197Y. The latter plasmid was microinjected into the eggs of *Drosophila* strain w^{1118}; *PΔ2–3 TM3 Sb/Dr* (8) to produce transgenic flies.

Protein Purification from E. coli—The expression of recombinant proteins was induced by adding 1 mM IPTG to the LB medium at 37 °C. Proteins were affinity-purified with nickel-nitrilotriacetic acid-agarose (Qiagen). The samples were at least 95% pure according to SDS-polyacrylamide gel electrophoresis. The concentration was adjusted to 0.01 mg/ml with PBS for spectroscopic measurements (see Fig. 1, *A* and *B*). Affinity purification of proteins from inclusion bodies was performed after three cycles of sonication-precipitation of lysate and further denaturation in 8 M urea. Protein concentrations were determined by a Bio-Rad protein assay kit.

Measurement—A Hitachi U-3400 spectrophotometer and a Hitachi 650–60 spectrofluorimeter were used for the absorbance and fluorescence measurements, respectively. All measurements were done at 25 ± 1 °C. For the green channel of DsRed and GFP, samples were excited at 470 and 480 nm, and emission was detected at 500 and 510 nm, respectively. For the red channel of DsRed, excitation and detection were performed at 555 and 585 nm.

Cell Culture and Lysate Preparation—For time course analysis (see Fig. 1*C*), *E. coli* carrying EGFP, wild-type DsRed (wtDsRed), or DsRed S197Y in the pET-11 plasmids were grown until OD = 1.0 (at 650 nm) in the presence of 1% glucose as suppressor of recombinant protein production. Transgene expression was induced by the resuspension into fresh LB medium containing 1 mM IPTG. Incubation was performed at 28 °C to make the experiment comparable with *Drosophila* culture cells. To prepare lysate, cells were collected by centrifugation at 0 °C, resuspended in ice-cold PBS, intensively sonicated on ice, cleared by centrifugation at 12000 × *g*, 0 °C, and adjusted to OD = 1.0 at 280 nm with PBS. The total delay from the beginning of lysate preparation to fluorescence measurements was within 30 min. To analyze temperature dependences of fluorescence maturation (see Fig. 1, *E* and *F*), *E. coli*

* This work was supported in part by an ERATO/JST grant (to S. T.), Human Frontier Science Program (HFSP), Monbu-Kagakusho, and PRESTO/JST grants (to K. I.), and a Core Research for Evolutional Science and Technology/JST grant (to M. Katsuki). The costs of publication of this article were defrayed in part by the payment of page charges. This article must therefore be hereby marked "*advertisement*" in accordance with 18 U.S.C. Section 1734 solely to indicate this fact.

§ To whom correspondence should be addressed: Tsukita Cell Axis Project, Kyoto Research Park, Shimogyo-ku, Kyoto 600-8813, Japan. Tel.: 81-75-315-7912; Fax: 81-75-315-9044; E-mail: vverkhus@cell.tsukita.jst.go.jp.

[1] The abbreviations used are: GFP, green fluorescent protein; IPTG, isopropyl-β-D-thiogalactopyranoside; BrdUrd, bromodeoxyuridine; MB, mushroom body; PBS, phosphate-buffered saline; wt, wild-type; kb, kilobase pair; EGFP, enhanced GFP; PCR, polymerase chain reaction.

cells expressing EGFP or DsRed S197Y were grown in anaerobic conditions for 3 days to disturb autoxidation of chromophore. For fluorescence development, air was admitted while lysing cells by intensive sonication on ice, followed by incubation at 4, 16, 25, 37, 53, 65, and 80 °C.

Culture and transfection of *Drosophila* S2 cells (see Fig. 1*D*) were carried out as described (9). To activate gene expression using the GAL4-UAS system (10), cells in 10-cm dishes were co-transfected with pWAGAL4 plasmid (a gift from Y. Hiromi, carrying GAL4 gene under cytoplasmic actin Act5C promoter) and pUAST-GFP S65T::actin (11; carrying GFP reporter gene fused with cytoplasmic actin gene), pUASp-DsRed, or pUASp-DsRed S197Y, in ratio 1:1, and incubated for defined hours at 25 °C. Cleared lysate (OD = 1.0 at 280 nm) was prepared and measured as above. Murine L cells (ATCC) were cultured in RPMI medium (Life Technologies, Inc.) supplemented with 10% fetal bovine serum (Sigma) at 37 °C and co-transfected with pWAGAL4 and either pUASp-DsRed or pUASp-DsRed S197Y, in ratio 1:1, using DMIRE-C reagent (Life Technologies, Inc.).

Confocal Microscopy—The *Drosophila* larval eye discs and brains were dissected in PBS, fixed with 4% formaldehyde/PIPES (100 mM)-EGTA (2 mM)-$MgSO_4$ (1 mM) buffer for 50 min, and mounted in 80% glycerol/PBS. 60–100 serial optical sections at 0.5 to 1-μm intervals were taken with a Zeiss LSM 510 confocal microscope and three-dimensionally reconstructed using BitPlane Imaris software. To minimize the cross-talk between GFP and DsRed signals and avoid reabsorption of GFP emission by DsRed, scanning is done separately using a 488-nm laser line and BP505–550 emission filter for GFP and 568-nm line and LP585 filter for DsRed.

RESULTS AND DISCUSSION

Molecular Characteristics of DsRed S197Y—DsRed S197Y showed 20% higher fluorescence intensity than the wtDsRed; Fig. 1*A*), although the wavelength of the peak shifted only by 2 nm (*i.e.* 585 nm). The level of excitation peak (558 nm) was also slightly enhanced. When excited within the 440–490-nm range, wtDsRed shows a significant secondary emission peak around 500 nm (Fig. 1*B*, *arrow*), which becomes a source of cross-talk with GFP imaging. DsRed S197Y almost completely suppresses this peak. The peak is not detected when wtDsRed is excited at the 310–350-nm range; *e.g.* see Fig. 1*A*.

The wtDsRed can take two energetically distinct states of chromophores, green (500 nm) and red (583 nm) (12). Because DsRed form tight tetramers (1, 13), a single tetramer may contain monomers with both green and red chromophores. Thus, the suppression of the 500-nm emission peak in DsRed S197Y might mean either a higher percentage of monomers that are matured to red state or a higher rate of intermolecular fluorescence resonance energy transfer from green monomers to red ones within the same tetramer or both.

When expressed in culture cells, DsRed S197Y exhibited a 3–3.5 times higher level of fluorescence than wtDsRed in both *E. coli* and *Drosophila* S2 cells (Fig. 1, *C* and *D*). Mammalian L cells also showed the relative fluorescence ratio of 3.4 ± 0.3 times. Because the differences are much bigger than the 20% fluorescence increase (Fig. 1*A*) per molecule, it is likely that more fluorescent protein exists in S197Y-expressing cells. In fact, a Bio-Rad assay of affinity-purified proteins showed that *E. coli* expressing DsRed S197Y produce 2.7 ± 0.2 more fluorescent protein than the cells that express wtDsRed. Because the expression-driving system is identical between wt and S197Y for each experiment, and the ratio of fluorescence intensity was rather consistent across culture systems, this increase may not primarily be because of the differences in transcription or translation levels.

Compared with *E. coli* that express DsRed S197Y, wtDsRed-expressing cells contained more than a 2 times higher amount of DsRed molecule in their inclusion bodies, which represents the active degradation process of intracellular proteins. It is thus likely that, similar to the GFP cycle 3 mutant (GFPuv) (14, 15), DsRed S197Y attained its stronger fluorescence mainly, because higher proportions of translated molecules are

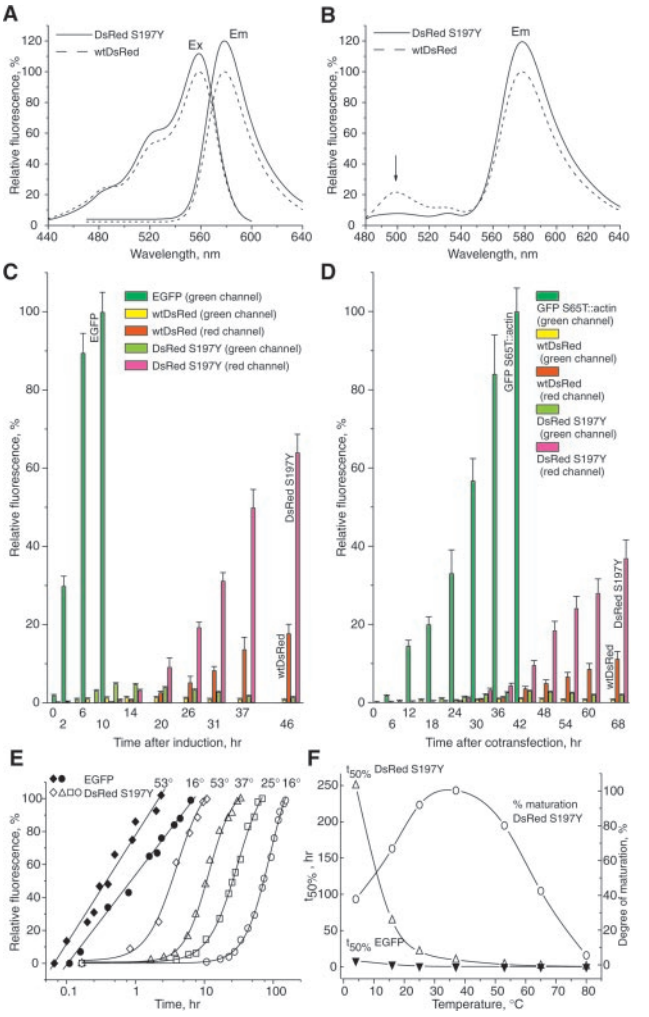

FIG. 1. **Intensity of DsRed S197Y fluorescence.** *A*, excitation (*Ex*) and emission (*Em*) spectra of wtDsRed (*dashed line*) and the DsRed S197Y mutant (*solid line*) in the mature state. Affinity-purified samples were excited at 330 nm for emission registration and detected at 630 nm for excitation spectra. The fluorescence peaks of wtDsRed were taken for 100%. *B*, emission spectra of affinity-purified wtDsRed (*dashed line*) and DsRed S197Y (*solid line*) excited at 470 nm. *Arrow*, suppression of emission peak between 480 and 540 nm. Fluorescence scale as in *A*. *C*, time course of fluorescence development (at 28 °C) in *E. coli* BL21(DE3) after induction of expression of EGFP, wtDsRed, and DsRed S197Y. Cleared lysate was prepared at various periods and subjected to fluorescence quantification. The maximal fluorescence of EGFP was taken for 100%. *D*, time course of fluorescence development (at 25 °C) in the *Drosophila* S2 cells after transfection of plasmid pUAST-GFP S65T::actin, pUASp-DsRed, and pUASp-DsRed S197Y, together with expression driver plasmid pWAGAL4. Lysate was used for quantification. The maximal fluorescence of GFP S65T::actin was taken for 100%. *E*, fluorescence development of EGFP (*solid symbols*) and DsRed S197Y (*open symbols*) at various temperatures. Intensities were normalized to 100% for maximum at each temperature and fitted by straight lines for EGFP and Boltzman curves for DsRed S197Y. *F*, time of half-maximal fluorescence maturation ($t_{50\%}$) of EGFP (*solid triangle*) and DsRed S197Y (*open triangle*), and degree of DsRed S197Y fluorescence maturation (*open circle*), at various temperatures. The $t_{50\%}$ data were fitted by exponential decay curves. For the degree of maturation, the peak fluorescence intensity achieved at 35 °C was taken for 100%.

folded properly and escape from the degradation process. Because the mutated 197th amino acid is oriented inside of the β-can structure of the DsRed protein, the difference is more likely to be because of the improved folding efficiency (3, 6) than because of the change in hydrophobisity or aggregation properties (15).

Maturation Process of DsRed S197Y—The development of DsRed fluorescence is much slower than EGFP (GFP F64L/

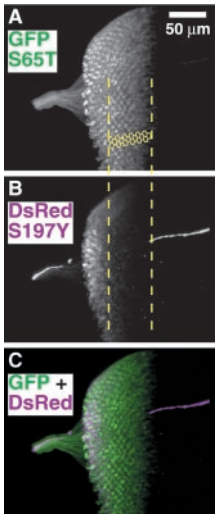

FIG. 2. **Developing eye disc of *Drosophila* expressing GMR-GAL4, UAS-GFP S65T, and UAS-DsRed S197Y transgenes.** Horizontal reconstruction of the eye disc of late third-instar larvae, anterior to the right. *A*, GFP S65T signal; *B*, DsRed signal; and *C*, composite. GFP, *green*; DsRed, *magenta* (used instead of *red* to ensure visibility for most color-blind readers). *Yellow hexagons* and *lines* indicate the rows of ommatidia cells that emit GFP signal but not DsRed. *Bright lines* in the DsRed image are the autofluorescence of tracheae visible at this wavelength. In the cells with DsRed signal, GFP tend to appear relatively weaker, presenting a *magenta* hue. This is partially because the intensity in the DsRed channel was enhanced to record fainter signals.

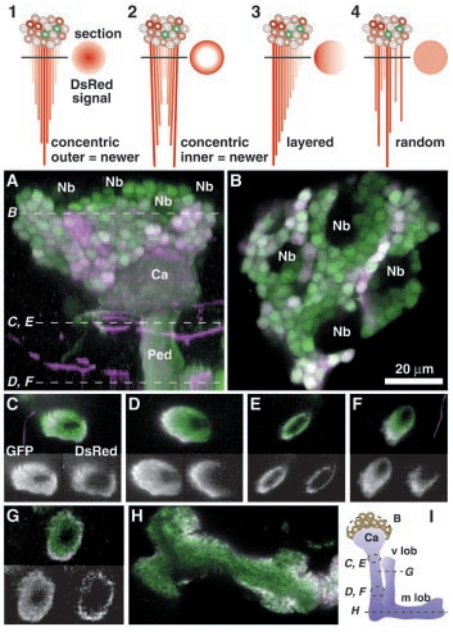

FIG. 3. **Formation order analysis of the larval mushroom body fibers.** *1–4*, possible cases of fiber bundle formation and the expected distribution of DsRed signal at the cross-section, in the case where DsRed expression begins at a relatively fixed period before or after the start of fiber extension. Various shades of *red* indicate the intensity of DsRed signal. *A-H*, GAL4 enhancer-trap strain *201y* with UAS-GFP S65T and UAS-DsRed S197Y. *A*, horizontal reconstruction of an MB at the end of the third larval instar. Anterior is to the bottom, and lateral is to the left. GFP, *green*; DsRed, *magenta*. *Nb*, neuroblast; *Ca*, calyx; *Ped*, pedunculus; *dashed lines* in *B–F*, positions of the vertical cross-sections in *panels B–F*. Notes on *magenta lines* and *magenta hue* are the same as in Fig. 2. *B*, vertical section near the surface of the cell body cluster. *C* and *D*, cross-sections of the pedunculus near its posterior root (*C*) and anterior end (*D*). *C–G* show the GFP (*left*) and DsRed (*right*) signals separately. *E* and *F*, cross-sections of respective ends at the early third larval instar. *G* and *H*, horizontal cross-sections of the vertical lobe (*v lob*; *G*) and medial lobe (*m lob*; *H*) at the end of the third larval instar. *I*, schematic diagram of the MB from the oblique frontal view. *Dashed circles B–F* and *dashed lines G* and *H*, positions of the vertical and horizontal cross-sections in *panels B–H*.

S65T) or GFP S65T (Fig. 1, *C* and *D*). The S197Y mutation did not change the maturation speed. The green fluorescence component of immature DsRed S197Y (Fig. 1, *C* and *D*, *yellow-green bars*) develops as rapid as GFP and then decreases. Its intensity is less than 6% of the GFP fluorescence even at its peak and less than 1% in the mature state, making the cross-talk with GFP signal practically negligible.

The fluorescence maturation curve in *E. coli* lysate was qualitatively distinct between EGFP and DsRed S197Y in a wide range of temperatures. In logarithmic plot of time, EGFP fluorescence increased linearly (Fig. 1*E*), which agrees with previously reported first-order kinetics (16). In contrast, DsRed S197Y showed remarkably sigmoid time dependences. This indicates that the red chromophore exhibits multi-stage maturation, which conforms to its suggested chromophore structure (12). The time for the half-maximum fluorescence development ($t_{50\%}$) decreases exponentially with temperature (Fig. 1*F*). The delay of $t_{50\%}$ between EGFP and DsRed S197Y is longer at lower temperature (empirical equation, $t_{50\%} = 238 \times \exp^{(4\ -\ t\ °C)/8.75}$). At 18, 21, 25, 28, and 37 °C, the delays are 48.1, 34.1, 21.6, 15.3, and 5.5 h, respectively.

The maximal level of DsRed S197Y fluorescence acquisition shows bell-shaped temperature dependence with its peak at around 35 °C (Fig. 1*F*). The final yield of fluorescence is irreversibly decreased at lower and higher temperatures. No further fluorescence growth was observed when samples kept at low or high temperatures were later transferred to 35 °C. The fluorescence did not decrease when the samples matured at 35 °C were transferred later to low or high temperatures either. These indicate that at least two processes affect the degree of DsRed S197Y maturation; one increases, and the other decreases the yield of maturated chromophore with temperature.

Double Labeling with DsRed S197Y and GFP S65T—For a practical use of DsRed S197Y, we made a *Drosophila* transformant strain carrying the transgene under GAL4-responsive sequence UAS. Various fly strains are widely available that carry fused GFP reporters under control of UAS, *e.g.* GAP::GFP (17), GFP::actin (11), and neuronal-synaptobrevin (vamp)::GFP (18, 19). The UAS-DsRed S197Y strain would be useful for counter staining the cells that are labeled with such GFP reporters.

The slow speed of DsRed fluorescence maturation has often been regarded as a drawback. We found that it is actually a beneficial feature for a fluorescent developmental timer. The red fluorescence of DsRed S197Y becomes visible much later than the green signal of GFP S65T (or EGFP) when they are expressed by the same promoter. If co-expression is activated shortly after the generation, or final differentiation, of certain types of cells, the fluorescence hue would reflect the order of their generation/differentiation.

To test whether this works practically, we expressed both GFP S65T and DsRed S197Y in the developing eye disc of *Drosophila* larvae (Fig. 2). Retinal cells are differentiated row by row immediately posterior to the morphogenic furrow, which moves from posterior edge of the disc to the anterior at the speed of ~1.5 h per row (at 25 °C) (20). When reporters were co-expressed by the driver strain GMR (glass multimer reporter)-GAL4, which drives expression in the differentiated cells posterior to the morphogenic furrow (21), the GFP signal appears a few columns behind the furrow. DsRed becomes visible about 12 rows behind (roughly corresponding to 18 h of delay). Because cells throughout retina emit both DsRed and GFP signals in later stages (not shown), the lack of DsRed signal in the green cells of the larval eye disc is not because of the failure of DsRed expression. Thus, the fluorescence hue reflected the

order of cell differentiation in this system.

Visualizing Formation Process of Mushroom Body Neural Fibers—A significant part of the brain consists of bundles, tracts, and meshwork of neural fibers. Investigating how such structures are composed is an important step for understanding the mechanism of brain development. How do neural fibers form bundles during neurogenesis? In the case where neurons start extending their fibers at a relatively fixed period after their generation, the order of fiber formation should correspond to the age of the cells. It was impossible to analyze the order even in such cases, because traditional birth-date analysis, labeling DNA-replicating cells with [^{3}H]thymidine or bromodeoxyuridine (BrdUrd), can visualize only nuclei. On the other hand, GFP and DsRed spread into cytoplasm of even fine cellular processes that are far from nuclei.

Using this approach, we analyzed the formation process of the fiber bundle of mushroom bodies (MBs). In *Drosophila*, four stem cells (neuroblasts) sequentially generate three major subtypes of MB neurons (Kenyon cells), which are in the adult innervate γ, α'/β', and α/β lobes, respectively (22, 23). The pedunculus of the adult MB has a concentric structure with the oldest γ lobe fibers running at the periphery and the youngest α/β lobe fibers occupying the core (18, 24). The formation order of fibers within each subtype, however, could not directly be investigated.

To visualize this process, we expressed GFP and DsRed in the larval MB using GAL4 enhancer-trap strain *201y* (25). This strain labels a large subset of Kenyon cells of the first subtype that form a γ lobe in the adult but innervate both vertical and medial lobes in larvae. In the cluster of cell bodies, neuroblasts, surrounding ganglion mother cells and newly generated neurons, are left unlabeled (Fig. 3, *A* and *B*). Neurons surrounding them emit only GFP signal, suggesting that they are shortly after the onset of reporter expression. Cells far from the neuroblasts emit both GFP and DsRed signals and are thus older. This age-dependent distribution agrees with the previous birth-date analysis using BrdUrd (26).

In the cross-section at the posterior root of the pedunculus, many fibers show only green GFP signal (Fig. 3*C*), indicating that *201y*-labeled cells extend their fibers well before DsRed signals become visible. DsRed-positive fibers, which should be older, are observed only in the periphery. Thus, it is likely that the larval pedunculus is ordered in a concentric manner according to their age, with younger fibers in the inner area (Fig. 3, *diagram 2*). A thin green layer appears in the fringe of the bundle, suggesting that a small subset of fibers extend along the outer surface of the bundle. The center of the bundle is unlabeled with both GFP and DsRed. They would correspond to the fibers of the unlabeled young neurons near the neuroblast (Fig. 3*B*), or certain cells that are not labeled with *201y* might form a specific structure at the core.

Near the anterior end of the pedunculus, DsRed-positive old fibers show crescent-like distribution but still remain in the periphery (Fig. 3*D*). During larval period, the number of Kenyon cells increase from 250 $\pm$ 50 to 1670 $\pm$ 176 (27). Accordingly, the cross-section of the pedunculus is much smaller in younger larvae. The concentric distribution of old and new fibers was identical even at these stages (Fig. 3, *E* and *F*). In the vertical and medial lobes, DsRed-positive fibers are observed only in the periphery (Fig. 3, *G* and *H*). Thus, throughout larval development, most of the newly projecting Kenyon cell fibers extend into inner part of the fiber bundles of pedunculus and lobes to shift older fibers outwards.

Another recently reported DsRed mutant, E5, which emits a strong green signal when immature (28), is also useful for such formation-order analysis. Unlike DsRed S197Y, E5 presents a different fluorescence hue without the help of co-expressed GFP. Its strong green signal at the constitutive expression state, on the other hand, makes it less suitable for double labeling with GFP-based reporters. DsRed S197Y can be used for dual purpose, fluorescent timer during development and counter stainer of GFP in the mature state. This is especially useful in systems like *Drosophila*, where introducing multiple reporters into one animal is an easy task by crossing various transformant lines.

Acknowledgments—We thank B. Dickson, M. Nakamura, D. Armstrong, and K. Kaiser for *Drosophila* strains and Y. Hiromi and P. Rorth for plasmids. We are indebted to M. Katsuki and Y. Nishida for generous support to make this collaborative project possible. We also thank E. Karbozova, P. Vrzheshch, K. Turoverov, H. Taguchi, and Y. Ohsumi for support, discussions, and suggestions. We are grateful to S. Okajima and M. Okubo for technical assistance.

REFERENCES

1. Baird, G. S., Zacharias, D. A., and Tsien, R. Y. (2000) *Proc. Natl. Acad. Sci. U. S. A.* **97,** 11984–11989
2. Matz, M. V., Fradkov, A. F., Labas, Y. A., Savitsky, A. P., Zaraisky, A. G., Markelov, M. L., and Lukyanov, S. A. (1999) *Nat. Biotechnol.* **17,** 969–973
3. Tsien, R. (1998) *Annu. Rev. Biochem.* **67,** 509–544
4. Fradkov, A. F., Chen, Y., Ding, L., Barsova, E. V., Matz, M. V., and Lukyanov, S. A. (2000) *FEBS Lett.* **479,** 127–130
5. Wachter, R. M., Elsliger, M. A., Kallio, K., Hanson, G. T., and Remington, S. J. (1998) *Structure* **6,** 1267–1277
6. Cubitt, A. B., Woollenweber, L. A., and Heim, R. (1999) *Methods Cell Biol.* **58,** 19–30
7. Rorth, P. (1998) *Mech. Dev.* **78,** 113–118
8. Robertson, H. M., Preston, C. R., Phillis, R. W., Johnson-Schlitz, D. M., Benz, W. K., and Engels, W. R. (1988) *Genetics* **118,** 461–470
9. Oda, H., Uemura, T., Harada, Y., Iwai, Y., and Takeichi, M. (1994) *Dev. Biol.* **165,** 716–726
10. Brand, A. H., and Perrimon, N. (1993) *Development* **118,** 401–415
11. Verkhusha, V. V., Tsukita, S., and Oda, H. (1999) *FEBS Lett.* **445,** 395–401
12. Gross, L. A., Baird, G. S., Hoffman, R. C., Baldridge, K. K., and Tsien, R. Y. (2000) *Proc. Natl. Acad. Sci. U. S. A.* **97,** 11990–11995
13. Vrzheshch, P. V., Akovbian, N. A., Varfolomeyev, S. D., and Verkhusha, V. V. (2000) *FEBS Lett.* **487,** 203–208
14. Crameri, A., Whitehorn, E. A., Tate, E., and Stemmer, W. P. (1996) *Nat. Biotechnol.* **14,** 315–319
15. Fukuda, H., Arai, M., and Kuwajima, K. (2000) *Biochemistry* **39,** 12025–12032
16. Reid, B. G., and Flynn, G. C. (1997) *Biochemistry* **36,** 6786–6791
17. Ritzenthaler, S., Suzuki, E., and Chiba, A. (2000) *Nat. Neurosci.* **3,** 1012–1017
18. Ito, K., Suzuki, K., Estes, P., Ramaswami, M., Yamamoto, D., and Strausfeld, N. J. (1998) *Learn. Mem.* **5,** 52–77
19. Estes, P. S., Ho, G. L., Narayanan, R., and Ramaswami, M. (2000) *J. Neurogenet.* **13,** 233–255
20. Wolff, T., and Ready, D. F. (1993) in *The Development of Drosophila melanogaster* (Bate, M., and Martinez-Arias, A., eds) Vol. II, pp. 1277–1325, Cold Spring Harbor Laboratory Press, Cold Spring Harbor, NY
21. Freeman, M. (1996) *Cell* **87,** 651–660
22. Ito, K., Awano, W., Suzuki, K., Hiromi, Y., and Yamamoto, D. (1997) *Development* **124,** 761–771
23. Lee, T., Lee, A., and Luo, L. (1999) *Development* **126,** 4065–4076
24. Crittenden, J. R., Skoulakis, E. M., Han, K. A., Kalderon, D., and Davis, R. L. (1998) *Learn. Mem.* **5,** 38–51
25. Yang, M. Y., Armstrong, J. D., Vilinsky, I., Strausfeld, N. J., and Kaiser, K. (1995) *Neuron* **15,** 45–54
26. Ito, K., and Hotta, Y. (1992) *Dev. Biol.* **149,** 134–148
27. Hinke, W. (1961) *Z. Morphol. Tiere* **50,** 81–118
28. Terskikh, A., Fradkov, A., Ermakova, G., Zaraisky, A., Tan, P., Kajava, A. V., Zhao, X., Lukyanov, S., Matz, M., Kim, S., Weissman, I., and Siebert, P. (2000) *Science* **290,** 1585–1588